NAVIGATING THE FUTURE: ADVANCEMENTS IN GPS ACCURACY

Aaron Becker
MIT Department of Mechanical Engineering
Cambridge, MA, USA

ABSTRACT

Global Positioning System (GPS) receivers are integral to a wide array of technologies we use every day, including automobiles, smartphones, and airplanes. Cutting-edge GPS receivers utilize advanced techniques to increase accuracy; Real-Time Kinematics (**RTK**), which refines accuracy using the satellite signal's carrier wave phase, as well as Internet-based **RTCM** (Radio Technical Maritime Commission) corrections to compensate for atmospheric effects. A U-Blox ZED-F9P GNSS module, with theoretical accuracy of 8 mm (0.008 m), was compared to an ultrasonic distance sensor with an accuracy of 1 mm (0.001 m) under three conditions: static receiver, small displacements of 20cm magnitude, and a single applied impulse along a low-friction dynamics track. RTK+RTCM correction improved the mean absolute error by a factor of 12 for the static experiment and a factor of 3 for the small displacement experiment. However, no statistically significant change in accuracy was observed with the impulse experiment (shortest timescale ~15 sec).

Keywords: GPS (Global Positioning System), GNSS (Global Navigation Satellite Systems), Geospatial Accuracy, Real Time Kinematics, RTCM Correction

INTRODUCTION

Modern Global Positioning System (**GPS**) receivers are pivotal in answering two fundamental questions – what is our current position, and how fast are we going? Given their widespread use, exploring ways to make this technology more accurate and more cost-effective are important open areas of research that will allow its adoption into an ever-growing number of use cases. Thus, understanding both the accuracy limitations of state-of-the-art, modern receivers, and the generational improvement over cheaper and older receivers is of paramount importance to determine the suitability of GPS technology in any given application. State of the art receivers are approximately three to five times as expensive but promise an accuracy increase of an order of magnitude, depending on the exact use case [1] [2].

The question about GPS accuracy is really one about noise – the satellite signals that allow the determination of position are inherently limited in their accuracy. Although synchronized nearly perfectly in space, as the signals travel through the atmosphere to a receiver on the ground they become less accurate: ionospheric, atmospheric, and relativistic effects all reduce signal strength and add uncertainty.

In the decades since the invention of GPS, several technologies have been developed to reduce this uncertainty, and thus improve real-time position and velocity solution accuracy. One technology, termed Real-Time Kinematics (**RTK**), uses the GPS receiver's measurements of the phase of the satellite signal's carrier wave to resolve ambiguities in the carrier signal, as well as receiving from multiple different GPS constellations at once to decrease the overall solution error. Another technology is called **RTCM** correction (Radio Technical Commission of Maritime Services), which helps to correct for local ionospheric and relativistic effects with ground-based stations near the receiver - the name being a nod to GPS's early adoption in the maritime industry. With these technologies, the cutting edge of modern receivers can achieve unprecedented absolute positional accuracies of ~10 centimeters or better [1].

To evaluate the suitability for different use cases, the impact of these advanced technologies can be quantitatively determined by examining the absolute accuracy of **GPS** alone versus **GPS+RTK+RTCM.** Accuracy is compared across multiple different experiments designed to simulate real-life conditions: static drift with no receiver movement, discrete small displacements of ~20cm, and an impulse experiment (which approximates constant velocity).

In all experiments, the position of a rover (moving target) on a low-friction track is first measured with a high-accuracy, localized sensor such as an ultrasonic distance sensor. These measurements are then be compared with the reported values from a receiver with and without **RTK+RTCM** corrections.

GPS data lends itself well to visualization; from the raw data a 3D point cloud of measured positions throughout each experiment can be plotted. This type of visualization not only aids in understanding the data but also reveals the 3D shape of the data's distribution, providing insights into dimensional accuracy (for example, altitude accuracy may be worse than horizontal accuracy). Then, by comparing the deviation in the residual between a reconstructed GPS position along the track, versus a ground truth high-accuracy, local sensor, the experiment is expected to highlight the inaccuracies of standalone GPS (greater then one meter) compared to the **GPS+RTK+RTCM** combination. The advanced technologies should be an order of magnitude better, thus justifying the additional cost and complexity of these systems when high accuracy is desired. Results will also be compared against historical GPS data and manufacturer specifications to validate the recorded data and confirm the accuracy improvement.

HISTORY OF GPS TECHNOLOGY AND BASICS

A brief history of the technology highlights the importance of this project: GPS was first invented in the United States by the Advanced Research Projects Agency (ARPA), mainly for military use in guiding missile submarines in the 1960s. However, its use was limited under a program termed Selective Availability (SA), which introduced intentional timing error into the system for non-military receivers to discourage use. The full details are beyond the scope of this paper, but the full-precision signal, transmitted in a frequency band termed L1, was initially only available to military receivers with a special encryption key. The transition to commercial use came in 2000, when the United States government disabled Selective Availability, which allowed civilian GPS receivers to receive the full-precision signal for the first time. Since then, because of its high accuracy, GPS has exponentially increased in popularity and receivers have been integrated into many billions of devices, such as the smartphone.

The beauty of GPS is its simplicity – at its core, it is a passive technology that scales extremely well because no additional investment is needed as receivers are added (since the signals are only one-way: from a small number of satellites orbiting Earth to many receivers on the ground). Fundamentally, this technology is based on simple physics – accurate timekeeping. GPS satellites orbiting Earth contain extremely accurate atomic clocks, which broadcast synchronized time signals down to Earth. These time signals are then received on the ground, with each signal arriving at the receiver at a slightly different time depending on the distance to the broadcasting satellite. These signals are then compared and triangulated to determine absolute position anywhere on Earth. However, ionospheric, atmospheric, and relativistic effects add noise to these signals, fundamentally impacting the accuracy achievable with satellite reception alone even with SA disabled.

TRANSMISSION FREQUENCIES (L1/L2/L5 BANDS)

In addition to correction technologies at the receiver, the GPS carrier signal itself has evolved in terms of the frequencies used. Today, there are three main frequencies, called "bands": L1, L2, and L5. The original L1 (1575.42 MHz) band is supported by essentially all receivers and contains the civilian and military signals required for basic GPS operation [4]. However, it was not optimized for range or power, and often suffers in environments like canyons, cities, and under challenging atmospheric conditions (cloud cover, thunderstorms) where the signal can be reflected or lost. This makes it unsuitable for aircraft, which often need the highest precision exactly *in* these challenging conditions, necessitating improvements in the underlying GPS technology.

The L2 band (1227.60 MHz) was originally intended for military applications only but was opened for civilian use when Selective Availability was disabled [4]. Receivers that support both the L1 and L2 frequencies can achieve higher accuracy because they can correct for some ionospheric error due to measuring the frequency difference between L1 and L2. Comparing the delay between the two frequencies allows the receiver to estimate this source of error, enabling higher accuracy.

Finally, the L5 band (1176.45 MHz) is the newest addition to GPS bands supported by the most recently launched satellites [4]. It was designed specifically for civil aviation, solving the issue with the L1 band mentioned previously. As an example of the power of GPS technology, its use is mandated by the Federal Aviation Administration in EGPWS (Enhanced Ground Proximity Warning Systems) in all commercial airliners. The aircraft's altitude and position are monitored with high accuracy, predicting potential collisions with terrain and other aircraft before they happen and thus greatly enhancing safety. To achieve this, the L5 band features higher power, greater bandwidth, and new modulation technique that offers improved performance in challenging, high noise conditions, like large cities.

In the context of this project, the state-of-the-art receiver chosen (U-Blox ZED-F9P-02B) supports the L1 and L2 bands, allowing for ionospheric error correction without any external input. An antenna that is also capable of receiving both bands and tested with this receiver (U-Blox ANN-MB-00) was carefully selected, ensuring that accuracy benefits of being able to receive both bands are maximized. An alternate triband receiver, capable of receiving L1, L2 and L5 signals (Unicore Communications UM980) was considered, but was rejected due to the large increase in receiver and antenna cost for only a marginal increase in predicted accuracy claims to 0.005 meters.

GPS COORDINATE FRAMES

The receiver is only one piece of the complete system – another key piece is what coordinate system the receiver is measuring in. There exist three common coordinate frames that are used to measure position: NED (North-East-Down), Latitude/Longitude/Altitude (Lat/Lon in short), and ECEF (Earth-Centered, Earth-Fixed). Choosing the correct coordinate system is key to the accuracy of GPS technology in a particular application, due to errors associated with coordinate system transformations and the inherent characteristics of each system. Errors can arise during the conversion between these coordinate frames due to approximations and the mathematical complexity involved. Thus, understanding all coordinate system choices, and choosing one appropriately is a key factor in overall GPS accuracy, and must be done correctly for every application.

NED (North-East-Down) is defined relative to a local tangent plane to the Earth's surface (user configurable) where position is reported as an offset to the start position. This is especially use for any system that needs to position anything with relative accuracy, such as a drone operating within a local environment. Using NED has less perceptible errors for local movements but can become problematic over larger distances or in regions near the poles, where all longitude lines converge (thus making the direction of "North" ambiguous).

Latitude/Longitude/Altitude is likely the best-known choice of coordinate frame - the position on the Earth's surface is given in terms of absolute angular measurements, where latitude represents angles north or south of the Equator and longitude represents angles east or west of the Prime Meridian. The problem with this is that the Earth is not a sphere – it has areas of local variation that would cause massive inaccuracies if not considered (imagine climbing Mount Everest, and your GPS receiver reported your position deviating by 500m due to the increased altitude). For this reason, by convention we use an oblate spheroid model of the Earth, most commonly WGS-84 (World Geodetic System 1984). WGS-84 specifies two primary measurements: the semi-major axis (equatorial radius) and flattening factor, which describes the extent of the pole-to-equator flattening, which compensate for the effects of local terrain features. The semi-major and semi-minor axes have been specified as exactly 6378137.0 m and 6356752.314 m respectively, an important value to know if you are converting values in this coordinate frame to another [5].

Finally, ECEF (Earth-Centered, Earth-Fixed) is another choice – here, the origin is given at the center of the earth fixed to the Earth's rotation, with coordinates being reported as a Cartesian X, Y, and Z offset from that origin. This is useful in circumstances when absolute position is needed but comes at some difficulty with calculations – measuring a single centimeter when the origin is at the center of the Earth requires high-precision floating-point calculations with minimum 64 bits, which may not be possible on older computer systems. Thus, despite its global consistency and precision, it can be computationally intensive to convert into more intuitively understandable formats like Latitude/Longitude/Altitude.

For this project, because relative distance in a Cartesian frame is the quantity of interest, the ECEF coordinate frame was chosen because it yields Cartesian X, Y, and Z positions directly from the receiver, without factoring in sources of error from the conversion (which would happen using Lat/Lon, due to the oblate spheroid model imperfectly modelling the true curvature of the earth). In addition to being more convenient, the ECEF coordinate frame has been shown to be more accurate for converging on navigational solutions [6]. Given this, the distance D_{meas} moved during an experiment is computed directly using the following equation:

$$D_{meas} = \sqrt{\left(x_f - x_i\right)^2 + \left(y_f - y_i\right)^2 + \left(z_f - z_i\right)^2}, \quad (1)$$

where D_{meas} is the distance from start to end point (in meters) where x_f, y_f, z_f represent a measured GPS position, and x_i, y_i, z_i represent the start position, all recorded in meters in the ECEF coordinate frame.

ADVANCED CORRECTION: RTCM AND NTRIP

The final key piece of the experimental setup is RTCM correction. The development of RTCM standards began in the 1980s to standardize the transmission of differential corrections for maritime navigation. The protocol allows local ground stations, which are fixed position, to transmit their estimates of ionospheric and relativistic errors at their location to a moving ship or rover. Although transmitted originally over radio signals, in the 21st century this protocol was adapted to modern technology with the introduction of NTRIP (Networked Transport of RTCM via Internet Protocol). As the title indicates, this protocol provides a standardized set of communications that allows a moving receiver connected to the Internet to receive corrections from one or many local ground stations. Today, NTRIP is much more widely used than the original RTCM – for example, cell phones use NTRIP to obtain correction data from cell towers on a periodic basis. The GPS receiver (ZED-F9P) used in this paper was connected via cellular hotspot to RTK2GO, an online, free service that streams live correction data to any receiver, with the closest local station being in Brookline, MA [3], and hundreds more local stations in every major state and most countries.

EXPERIMENTAL DESIGN: LOW-FRICTION CART

For this experiment, the primary apparatus (Figure 1) consisted of a Vernier Dynamics Cart and Track System. This system was chosen for its low-friction characteristics, which are crucial for minimizing external variables that could skew the measurements of relative motion and distance. The track was also levelled by thumb screws at each end (secured by 8-32 nuts) and checked with a smartphone inclinometer, resulting in a cart that didn't slide to one side or another when placed on the track.

The low-friction cart (Figure 1, below) facilitates smooth and consistent movement along the track, allowing for more accurate and repeatable position data collection. Kinetic variables measured (such as acceleration and velocity) are not significantly affected by frictional forces, which is essential to evaluating the GPS system's ability to detect small positional changes. The ZED-F9P GPS sensor has a theoretical accuracy of 8mm (0.008mm), and the Go!Motion ultrasonic sensor has an accuracy of 1mm (0.001mm), enabling a comparison between the GPS measurements and its highly accurate local estimate for further analysis at a recording frequency of 20 Hz (GPS maximum solution update rate.

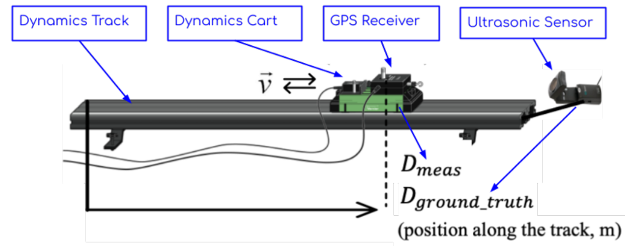

Figure 1: Diagram of experimental setup, showing low-friction track, cart, and GPS receiver attached to cart. As the cart slides along the track, the position is measured both with a local ultrasonic sensor and the GPS.

DESIGN OF RECEIVER PROCESSING HARDWARE

The experimental setup incorporated several off-the-shelf components configured around the selected GPS receiver, the U-Blox ZED-F9P, to process the raw GPS data effectively. Data recording and storage of runs utilized a Vernier LabQuest 3, which has four analog channels to capture the X, Y, and Z positions in the ECEF coordinate frame, as well as the velocity once they have been converted into analog signals. An additional digital channel was used for the Vernier Go!Motion ultrasonic distance sensor. The GPS signal conversion for the LabQuest 3 was facilitated by a Digital to Analog Converter (DAC), specifically the MCP4728 from Adafruit. The MCP4728 was chosen because of existing publicly available libraries to communicate with it over I2C, a widely used sensor protocol. Furthermore, an ESP32-S2 System on a Chip (SoC) was employed to manage multiple tasks: receiving RTCM correction signals via Wi-Fi, outputting data to the DAC, and processing incoming data from the GPS. The ESP32-S2 is notable for its integrated TCP/IP stack, which enables it to connect to a cellular hotspot for receiving correction data. All programming was done in C++, ensuring efficient handling of the data flow and system operations. See Appendix A for the full open-source code listing.

This combination of hardware and software supports a robust platform for capturing and analyzing GPS data under varied experimental conditions. Finally, the internal state of the system was displayed on a 20x4 character LCD (also using I2C), which improved the repeatability between experiments because the start conditions could be matched.

These components, and their interconnections are displayed in the system-level block diagram (Figure 2a) below.

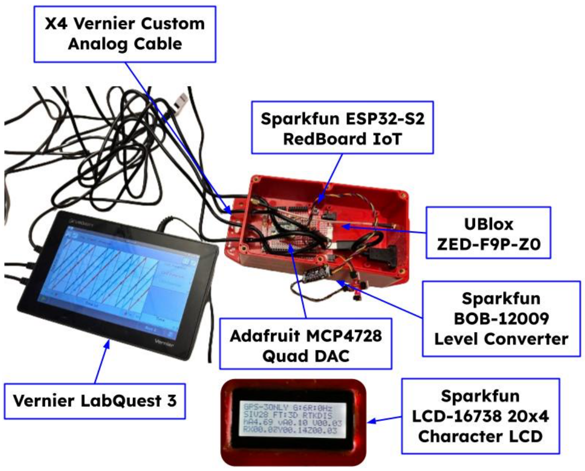

Figure 2a: Diagram of components in GPS receiver postprocessor box, showing DAC, ESP32 SoC, LabQuest 3, along with 20x4 character LCD for outputting status messages to the user.

Additionally, a data flow diagram (Figure 2b, below) illustrates how different sources interact inside the receiver box to improve accuracy. This diagram details the pathways from the RTCM/NTRIP endpoint (via a cellular hotspot), through the Go!Motion and U-Blox sensors, to the processor box, and finally to the LabQuest 3.

Figure 2b: Block flow diagram of data flow in receiver box, showing RTCM/NTRIP endpoint (cellular hotspot), Go!Motion and U-Blox sensor, processor box and LabQuest 3. RTCM correction data is streamed via cellular hotspot to ESP32-S2 inside data processor box.

Additionally, the DAC was validated using a triangle waveform of different amplitudes and the same period to ensure that all channels were responding appropriately. This was also used to test the postprocessor software, simulating a GPS displacement of 1, 2.25, 3.5, and 4.5 meters respectively in Figure 3 below.

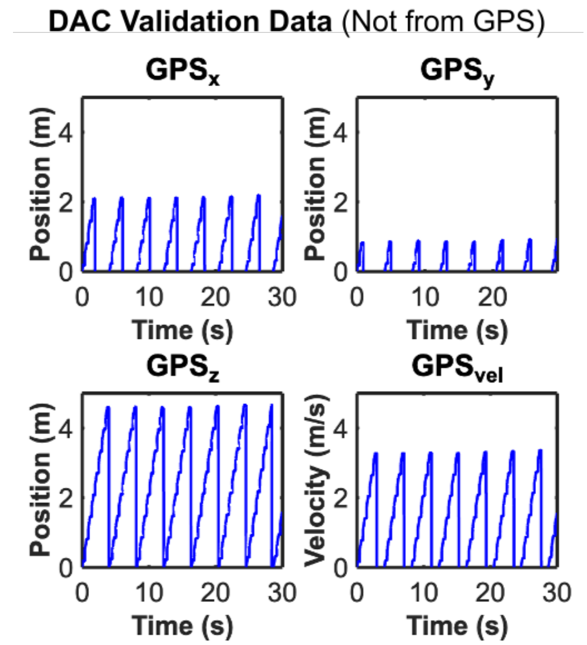

Figure 3: DAC validation waveform reconstructed through GPS postprocessor software, written in MATLAB. This test script simulated GPS displacements of 1, 2.25, 3.5, and 4.5 meters, which confirmed the hardware and software worked before adding further complexity. Note that the small dimples in the otherwise pure triangle wave are from hardware interrupts at 1Hz from the GPS unit. The DAC subroutine runs at a lower priority, and thus is temporarily paused in execution while the GPS code runs (yielding the dimples). In a real experiment, this would not be an issue because the data would only update as quickly as the GPS unit does.

GPS RECEIVER STATE MACHINE

In addition to processing the data, the receiver implements a simple state machine to determine readiness to conduct an experiment based on specific conditions, a key component to achieve high accuracy under constantly changing satellite conditions. The criteria are as follows:

- $GPS_{ready} = 1$
  - Indicates that the GPS is operational, and its ready bit is set.
- $Time_{current} - Time_{start} > 600sec$
  - Enforces a 10 minute warm-up period at the start of every experiment, to allow the GPS to converge.

- $Time_{current} - RTCM_{last_{received\_time}} < 10sec \lor RTCM_{enabled} == 0$
  - Indicates that RTCM data was received within the last 10 seconds, or that RTCM/RTK is disabled.
- $GPS_{positional\_accuracy} < 10.0\ m$
  - Indicates that the positional accuracy is within 10 meters (a check on solution convergence). This is a value reported by the receiver itself – not a statistical method performed on the data.
- $GPS_{velocity\_accuracy} < 5.0\ m$
  - Indicates that the velocity accuracy is within 5 meters (another check on solution convergence). This is also a value reported by the receiver itself – not a statistical method performed on the data.
- $GPS_{fixtype} == 3D \lor GPS_{fixtype} == RTK$
  - Ensures that the GPS has a full 3D fix, or an RTK fix. Some simplification here, because there are multiple different kinds of RTK fixes (floating, or fixed), but any kind of RTK fix is enough to perform an experiment.
- $GPS_{siv} > 15$
  - A minimum of 15 satellites must be in view of the receiver to achieve high accuracy. During the experiments, it was determined that 15 satellites serve as a practical threshold, given that typically at least 30 satellites were visible after the unit had been active for an extended period. It is important to note that a full assessment of satellites in view requires at least 12.5 minutes to acquire the latest ephemeris (orbit) data. However, a duration of 10 minutes with at least 15 satellites in view was found to be sufficient to attain the necessary accuracy for these trials.

Finally, this was visible to the operator using the 20x4 character LCD display. Additional complexity includes determining whether an RTK/RTCM connection has been established, and falling back to a non-RTK fix if the connection is lost. No data is output to the ADC channels until all readiness conditions are met, ensuring that all data measured was done under the most controlled conditions possible.

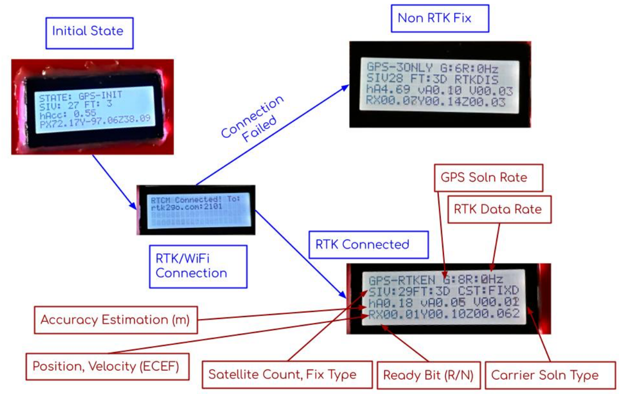

Figure 4: A simplified state machine diagram of the display visible to the user, including the transitions between RTK and non-RTK modes. Additionally, convergence characteristics are visible on the display, including many of the parameters that factor into readiness (all conditions being met indicated by Ready Bit, bottom). This allows live assessment of convergence during experiment set-up and ensures experimental results are consistent between trials.

EXPERIMENTAL METHOD

This study conducted three main experiments to assess GPS accuracy. The first was a static trial, where the receiver remained stationary, and any deviation from the initial position was measured over a 5-minute period (300 seconds). The objective was to gauge the stability of the GPS readings when the receiver is unmoved.

The second experiment involved discrete displacement trials. Here, the cart was manually moved by 20cm every 60 seconds, for a total displacement of up to 1 meter. This trial was designed to test the receiver's capability to accurately measure changes in position at the decimeter level. Human error in the 20cm measurement is not a factor in the results because the residual between the local sensor and GPS measurement is what was used in the computation of accuracy (meaning any error in human positioning of the cart was captured by the local sensor).

The third experiment was an impulse trial, where a preloaded spring was used to propel the cart. This setup allowed the cart to quickly traverse the entire meter of the track in less than 10 seconds, testing the receiver's ability to track sudden movements.

All three trials allow assessing different modes of the GPS units' performance that may be applicable to specific applications, because the performance may vary depending on the input condition being measured.

For all experiments, the embedded software in the processor box initiated a mandatory 10-minute warmup period at the start of each experiment. Between trials, the experiments were reset by issuing a serial command to the processor box, ensuring that each trial started under similar conditions. Trials were performed in sequence to get as close to identical satellite conditions as is feasible. A minimum of three trials per experiment was run to minimize the impact of outliers.

RESULTS AND DISCUSSION: ANALYSIS METHODS

After data collection for the three experiments was complete, various statistical methods for analyzing GPS data were evaluated. The primary concern in data analysis was that each GPS measurement is influenced by all preceding measurements, a dependency not readily characterized due to a multitude of factors, such as the dynamic positions of satellites throughout the course of a single run. Therefore, instead of evaluating uncertainty by combining multiple experimental runs, the mean residual (error) and variance are computed for each run explicitly. Then, a two-sample T-test ($\alpha = 0.1$) is performed on the corrected (RTK+RTCM) versus uncorrected (GPS only) experimental run residual means to ascertain whether there was in statistically significant difference between the accuracy with and without correction.

First, the absolute residual function $r(t)$ is defined, with D_{meas} being the GPS-measured position along the track computed using Equation 1, and D_{ground_truth} being the position along the track from the ultrasonic sensor. The absolute residual was chosen because the quantity of interest is the net deviation from the ground truth position over the course of an entire run, regardless of which direction that deviation is. Thus, $r(t)$ can be thought of as a measure of overall error for the GPS system.

$$r(t) = \left|D_{meas} - D_{ground_{truth}}\right| \tag{2}$$

A single trial run from the discrete displacement experiment is shown below in Figure 5 to illustrate the residual function $r(t)$ and the two signals.

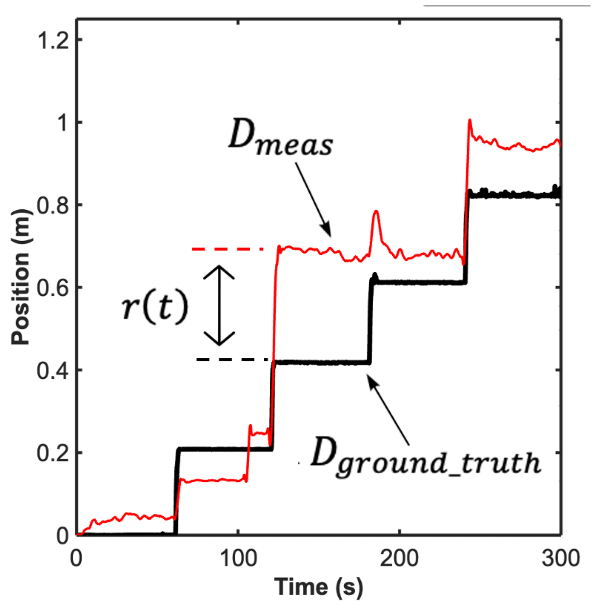

Figure 5: Single trial run of discrete displacement experiment plotted. Position refers to position along track, measured from cart starting position. Black line represents ground truth position along track from the Go-Motion sensor. Red line is the time-synchronized GPS position along the track, with RTK+RTCM correction applied. Observation of the y-axis scale shows alignment to ground truth to within 0.25 meters during the run, demonstrating the accuracy of the RTK+RTCM correction.

Next, the mean $E\big(r(t)\big)$ of this absolute residual function was computed with the following formula, for each run independently:

$$\mu_{|r(t)|} = \int r(t)dt \cdot \frac{1}{T_{final} - T_{initial}} \tag{3}$$

Then, the variance, $E\left(\left(r(t) - \mu_{|r|}\right)^2\right)$, or σ^2 was computed with the following formula, again for each run independently:

$$\sigma^2_{|r(t)|} = \frac{\int_{T_i}^{T_f} \left(r(t) - \mu_{|r|}\right)^2 \cdot dt}{T_{final} - T_{initial}} \tag{4}$$

The standard deviation is just the square root of the variance:

$$\sigma_{|r(t)|} = \sqrt{\sigma^2_{|r(t)|}} \tag{5}$$

RESULTS – EXPERIMENT 1 (STATIC)

During the static trial, the receiver was held stationary and measured over an interval (300 seconds, or 5 minutes) to assess its drift. In Figure 6 below, three runs of uncorrected, GPS only measurements (in blue) are compared to the same measurements using RTK+RTCM correction (in red). For this experiment, no residual plot was needed, since the expected position along the track should be zero throughout the duration of the experiment.

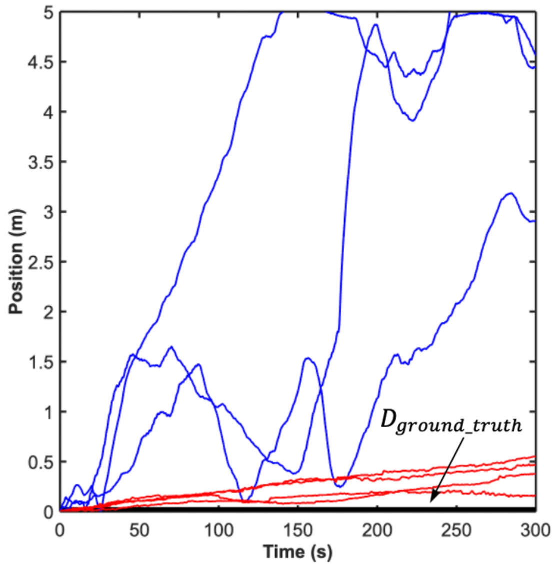

Figure 6: Results from static trial (receiver stationary), with uncorrected, GPS-only results in blue and RTK+RTCM corrected results in red, as well as the ground truth position indicated in black. The uncorrected residual experiences drift over this time interval to the high limit of 5 meters, which is likely undesirable for ground-based receiver applications.

In addition, the 3D ground track in the ECEF coordinate frame has been computed, shown in Figure 7. This shows the 3D shape of the data collected from the receiver.

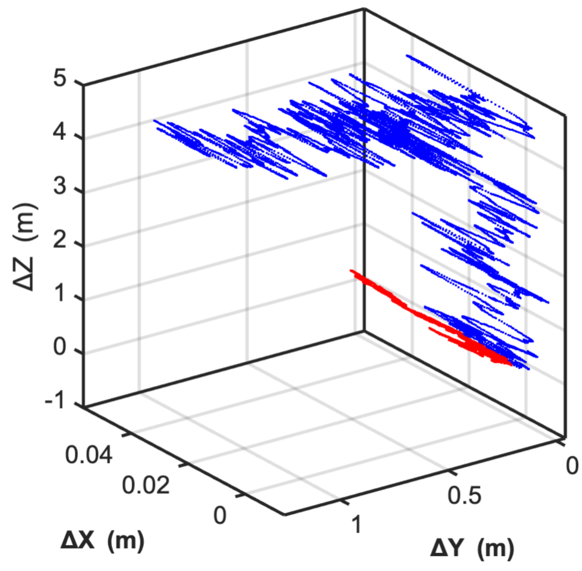

Figure 7: Reconstructed ground track of receiver position for static trials. Red is corrected RTK+RTCM, blue is uncorrected GPS only (as above). We can see that for both cases, vertical positional drift appears to be more significant than horizontal drift, a result expected due to the angle between receiver and satellite being harder to determine as satellite passes overhead. Additionally, the larger positional drift over time of the uncorrected signals is readily visualized.

To determine whether these results demonstrate a statistically significant difference, a T-test was carried out on the average absolute residual from each run, grouped into corrected and uncorrected populations with $\alpha = 0.1$. This is shown in Figure 8 below.

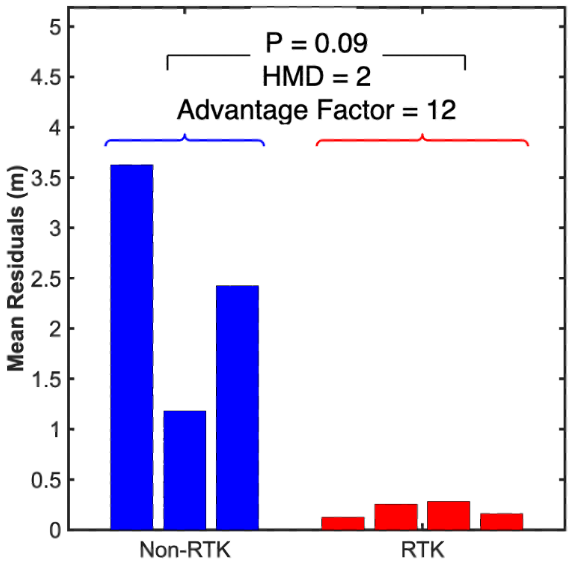

Figure 8: T-test results from static trial, with three uncorrected (Non-RTK) runs and four corrected (RTK+RTCM) runs. The P-value is 0.09, which is less than our chosen $\alpha = 0.1$, and thus we can conclude that there is a statistically significant difference in the populations. Moreover, the Hypothesized Mean Difference (HMD) between the two populations is 2, which corresponds to a 12-fold improvement in accuracy when using corrected data for a static application.

RESULTS – EX. 2 (DISCRETE DISPLACEMENT)

During the discrete displacement experiment, the receiver was moved in small 20 centimeter increments every minute. In Figure 9a below and on the left, three runs of uncorrected, GPS only measurements (in blue) are compared to the same measurements using RTK+RTCM correction (in red), as well as the ground truth cart position. In Figure 9b on the right, the absolute residual $r(t)$ between the GPS measured track position and the real position is shown.

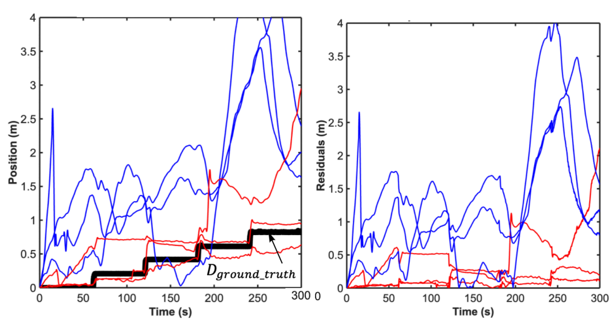

Figure 9a, 9b: Results from discrete displacement trial, with left graph showing the time series position along the cart track as a function of time. Red is RTK+RTCM, blue is uncorrected GPS only, and black is the ground truth position. The right graph is the time series absolute residual of the cart position, which quantifies the absolute deviation from the ground truth position. Both corrected and uncorrected data does show a spike in residual error after a displacement, but uncorrected data accumulates the error over time, by the end of the experiment demonstrating a large error from the true position.

In addition, the 3D ground track in the ECEF coordinate frame has been computed, shown in Figure 10 below. This shows the 3D shape of the data collected from the receiver.

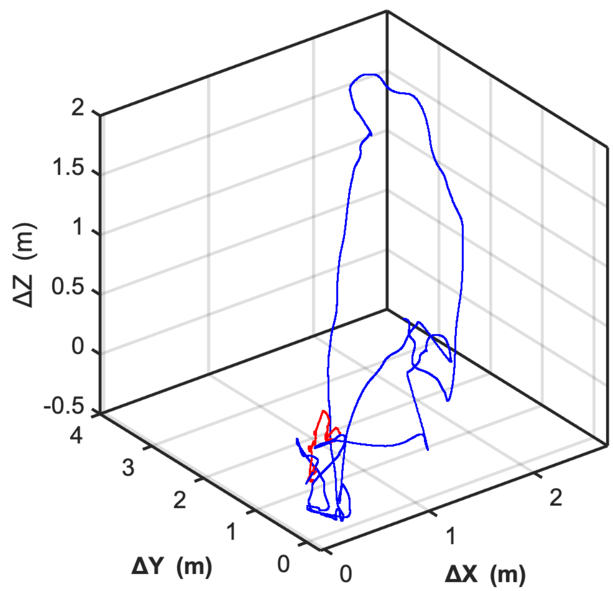

Figure 10: Reconstructed ground track of receiver position for discrete displacement trial. Uncorrected data in blue, corrected RTK+RTCM data in red. Corrected data visually stays within a much tighter bound around the origin position as compared to the uncorrected data.

Finally, in Figure 11 below, a T-test was again carried out on the average absolute residual from each run, grouped into corrected and uncorrected populations with $\alpha = 0.1$ to determine if there is a statistically significant result.

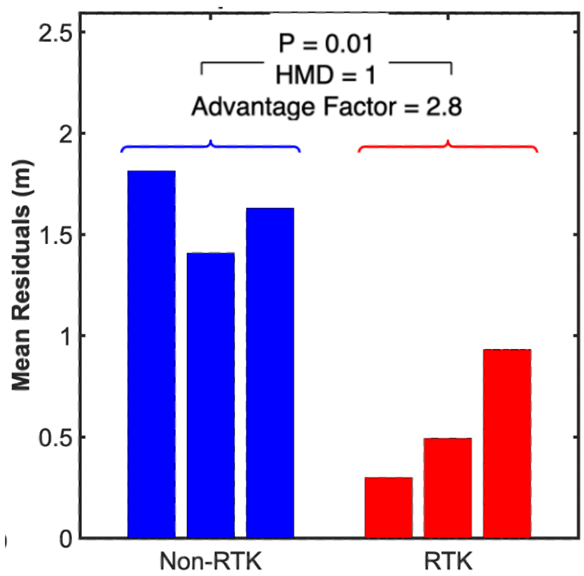

Figure 11: T-test results from discrete displacement trial, with three uncorrected (Non-RTK) and corrected (RTK+RTCM) runs. The P-value is 0.01, leading us to conclude that there is a statistically significant difference in the populations. The Hypothesized Mean Difference (HMD) between the two populations is 1, which corresponds to an approximately 3-fold improvement in accuracy when using corrected data for small, slow displacements.

RESULTS – EXPERIMENT 3 (IMPULSE)

During the impulse experiment, the cart started stationary on one end of the track before an known impulse was applied with a spring, causing it to travel at roughly constant velocity to the end of the track before bouncing off the end. In Figure 12a on the left, three runs of uncorrected, GPS only measurements (in blue) are compared to the same measurements using RTK+RTCM correction (in red), as well as the ground truth cart position. In Figure 12b on the right, the absolute residual $r(t)$ between the GPS measured track position and the real position is shown.

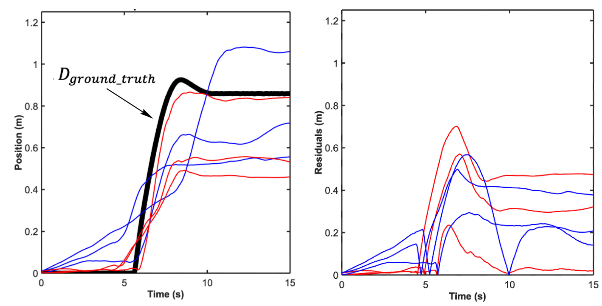

Figure 12a, 12b: Results from impulse trial, with left graph showing the time series position along the cart track as a function of time. Red is RTK+RTCM, blue is uncorrected GPS only, and black is the ground truth position. The right graph is the time series absolute residual of the cart position, which quantifies the absolute deviation from the ground truth position. Both show a large spike in error after the cart is displaced, which does decrease toward a constant value at the end of the data collection period. This is hypothesized to be because the RTK+RTCM algorithms take some time to resolve the new position by solving for ambiguities in the carrier signal, and there isn't enough time for them to be effective over only fifteen seconds of captured data and a large displacement.

In addition, the 3D ground track in the ECEF coordinate frame has been computed, shown in Figure 13 below. This shows the 3D shape of the data collected from the receiver.

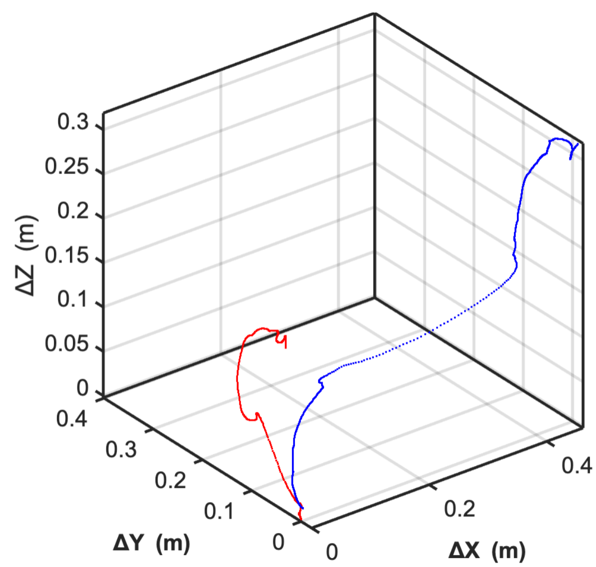

Figure 13: Reconstructed ground track of receiver position for impulse trial. Uncorrected data in blue, corrected RTK+RTCM data in red. Uncorrected data notably more deviation visually than corrected data.

Finally, in Figure 14 below, a T-test was again carried out on the average absolute residual from each run, grouped into corrected and uncorrected populations with $\alpha = 0.1$ to determine if there is a statistically significant result.

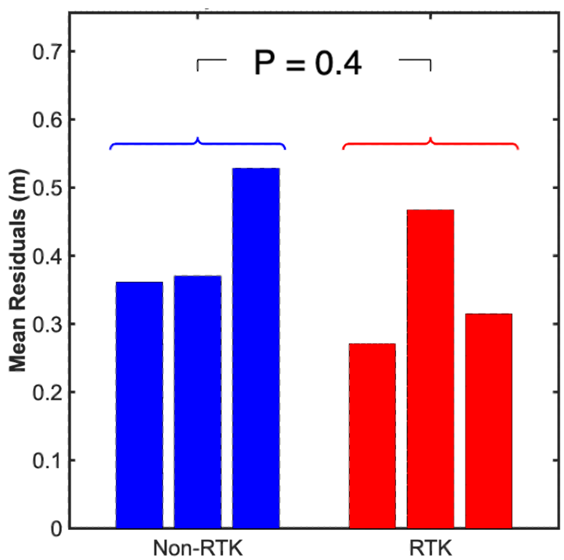

Figure 14: T-test results from impulse, with three uncorrected (Non-RTK) and corrected (RTK+RTCM) runs. The P-value is 0.4, leading us to conclude that there is no statistically significant difference in the populations and thus no accuracy improvement from using RTK+RTCM for this scenario.

DISCUSSION OF RESULTS

Additionally, the results are validated by previous work. In one previous study done exploring the use of an RTK+RTCM receiver on a moving rover (car) using a local correction station and NTRIP, the RTK fixed solution was preserved 96.9% of the time throughout a varied driving route including bridges, forests, and highway driving, which enabled centimeter-level accuracy [7]. This test is similar to the experiments in this paper, as it involves a moving rover using NTRIP-based corrections, with an RTK-enabled. In addition, all the issues that were encountered in their setup, such as trees blocking the source of the correction data causing a RTK solution loss are also issues in these experiments. The absolute accuracy of their measurements is shown in Table 1 below.

Table 1: Results from Uradzinski et. al [7], showing the accuracy of their GPS+RTK+RTCM receiver during a “varied course” driving test versus a ground-truth odometer solution, which included highway driving, forested driving, and bridge crossings. All values measured in meters in the ECEF coordinate frame. Average accuracy was far better then standalone GPS (3m nominal), with average deviation from truth ground track in the centimeter range, similar to the data for longer time scale experiments. Note that the Y axis was fixed to the vertical axis of the vehicle, which also shows a higher standard deviation as expected. RTK fixed solution maintained for 96.9% of test drive, with the remaining ~3% being predominantly under bridges, when the internet connection (and thus NTRIP) correction data lost.

	dx(m)	dy(m)	dz(m)
MIN	-0.366	-0.483	-0.251
MAX	0.196	0.146	0.356
AVERAGE	0.005	-0.011	0.012
STDEV	0.026	0.074	0.065

Uradzinski et. al also makes mention of other potential accuracy improvements in the system, where further research may be warranted. In particular, the GPS itself has many more configurable parameters then there was time to explore, including an internal model for the expected motion of the receiver through an Extended Kalman Filter, which allows further reduction in error if well-tuned. Tuning these parameters could yield better results for cases like the impulse results. More detailed analysis of satellite conditions could help narrow down when the best times for data collection would be, with the most satellites in view of the receiver. Adding even more cost and complexity to get a receiver and antenna capable of receiving the L5 band signal could also improve the accuracy. And finally, using multiple receivers (a technique known as Differential GPS) can also improve the accuracy, at the expense of cost and complexity.

CONCLUSIONS

The findings from both the static and discrete displacement trials indicate a marked enhancement in measurement accuracy when employing RTK+RTCM. Specifically, in the static trials, the error (measured as mean absolute residuals) were reduced by an impressive 12-fold using RTK+RTCM correction, with a statistically significant P-value of 0.09. In the discrete displacement trials, the error improvement was approximately 3-fold with a statistically significant P-value of 0.01. However, the results from the impulse trials did not demonstrate a statistically significant improvement, with a P-value of 0.4, indicating no substantial accuracy gain between the corrected and uncorrected data.

The lack of improvement in the impulse trials suggests that the benefits of RTK+RTCM corrections may be limited in dynamic environments where measurements are taken over brief periods. This observation is crucial for applications that involve rapid movement, where the addition of RTK+RTCM may not provide sufficient accuracy improvements to justify the increased complexity and expense. Conversely, for sectors requiring prolonged high precision, such as in automotive or aviation applications, the benefits of RTK+RTCM are clearly advantageous. These findings highlight the need for tailored application of RTK+RTCM technologies based on specific operational requirements and the dynamics of the target environment. Future research should explore the boundary conditions under which RTK+RTCM corrections are most effective, particularly focusing on quantifying factors that influence accuracy in time-dependent data.

ACKNOWLEDGMENTS

The author would like to thank Dr. Barbara Hughey, Dr. Will Li, and Dr. Dave Larson for their advice and feedback on the experiment and subsequent data analysis.

APPENDIX A – CODE LISTING

All C++ code written for this project is completely open-source and available online. If you would like to access it, please see this link to GitHub, which contains the full source code:
https://github.com/aaroexxt/MIT2.671/blob/main/GPS/GPS.ino

REFERENCES

[1] u.Blox, "ZED-F9P Module Specifications," 2024. Available: https://www.u-blox.com/en/product/zed-f9p-module [Accessed April 24, 2024].

[2] u.Blox, "NEO-M8N Module Specifications," 2024. Available: https://www.u-blox.com/en/product/neo-m8-series [Accessed April 24, 2024].

[3] *RTK2GO Service* (2024). *RTK2GO.* Available at: http://rtk2go.com/how-it-works/ [Accessed: 24 April 2024].

[4] J. Leclère, R. Landry Jr., C. Botteron, "Comparison of L1 and L5 Bands GNSS Signals Acquisition," Sensors, vol. 18, no. 9, pp. 2779, September 2018.

[5] T. Moore, V. Ashkenazi, M. Dumville, "Implementation of WGS84 and GPS for Marine Navitation", *International Hydrographic Review,* vol. 2, no. 1, Jan. 2001.

[6] A. Centinello III, "Analysis of the NED and ECEF Covariance Propagation for the Navigational Extended Kalman Filter", *Proceedings of the 58th International Astronautical Congress*, September 2007.

[7] Uradzinski, Marcin, Kim, Don, Langley, Richard B., "The Usefulness of Internet-based (NTrip) RTK for Navigation and Intelligent Transportation Systems," Proceedings of the 21st International Technical Meeting of the Satellite Division of The Institute of Navigation (ION GNSS 2008), Savannah, GA, September 2008, pp. 1437-1445.